

## **On the passive limited slip differential for high performance vehicle applications**

GADOLA, Marco, CHINDAMO, Daniel and LENZO, Basilio  
<<http://orcid.org/0000-0002-8520-7953>>

Available from Sheffield Hallam University Research Archive (SHURA) at:  
<http://shura.shu.ac.uk/21372/>

---

This document is the author deposited version. You are advised to consult the publisher's version if you wish to cite from it.

### **Published version**

GADOLA, Marco, CHINDAMO, Daniel and LENZO, Basilio (2018). On the passive limited slip differential for high performance vehicle applications. In: 14th International Symposium on Advanced Vehicle Control, AVEC 2018, Beijing, China, 16-20 July 2018. (In Press)

---

### **Copyright and re-use policy**

See <http://shura.shu.ac.uk/information.html>

# On the Passive Limited Slip Differential for High Performance Vehicle Applications

Marco Gadola\*, Daniel Chindamo\*, Basilio Lenzo\*\*

\* Dept. of Industrial and Mechanical Engineering, University of Brescia, Italy

\*\* Dept. of Engineering and Mathematics, Sheffield Hallam University, Sheffield, UK

E-mail: [marco.gadola@unibs.it](mailto:marco.gadola@unibs.it)

The paper is aimed at a comprehensive revision of the working principles and limitations of the mechanical limited slip differential, the traditional, passive device used to improve traction capabilities and to extend the performance envelope of high performance road cars, racing and rally cars. Its impact on vehicle handling through a yaw moment generated with passive torque distribution across the drive axle is investigated by means of vehicle dynamics simulations.

Topics / Vehicle Dynamics and Chassis Control; Torque Vectoring

## 1. INTRODUCTION

The limited slip differential (LSD) has been in use for decades, however its impact on vehicle dynamics is somehow neglected in literature. Current research on the subject of yaw control is usually focused on side aspects and/or on modern control applications like active differentials and torque-vectoring systems. These state-of-the-art technologies still rely on the same principles of the LSD, which should therefore be fully explained.

After an extensive literature review the paper provides an explanation of how a typical passive LSD can affect vehicle behaviour by using math models and examples, with the aim of filling the gap encountered in the related literature. The peculiar shape of the torque-sensitive LSD working zone on the torque bias diagram is explained in detail.

## 2. OVERVIEW

Differential (diff) locking can help to solve traction problems on low friction surfaces. It can also help to improve cornering behaviour and stability through the development of a yaw torque with a direct impact on handling characteristics, especially on high-performance vehicle applications with a high power-to-weight ratio.

Passive LSD devices are usually classified as speed-sensitive (the locking torque is a function of wheel speed difference, where a viscous cartridge is fitted in parallel with an open differential for instance) or torque-sensitive: the locking action is proportional to input torque, like in the so-called ramp diff. These devices are now superseded by actively controlled differentials or torque vectoring systems. However the use of passive limited-slip devices is still widespread where a back-to-basics driving experience is the key to marketing success, such as on lightweight sports cars, and even in professional motorsport: examples are championships like Formula 2 and 3 as well as Endurance racing. Nevertheless the LSD is still a fairly unknown or misunderstood device. One of very few experimental works dedicated to LSD characterization in motorsport is [29].

A literature survey over more than 40 years of research resulted in just a few papers dealing with the passive LSD. The most significant ones are mentioned here. An early experimental campaign conducted by a major manufacturer is [1], comparing free vs fully locked vs viscous vs ramp differential in terms of traction, braking and handling, including steering pad testing, throttle-off manoeuvres and frequency response analysis. [6] discusses passive LSD's for FWD cars. The interaction of torque biasing with steering geometry and suspension elasto-kinematics is also investigated. A detailed analysis on the behaviour of LSD-equipped RWD cars is [2], stating that suspension setup should be tuned according to LSD influence on handling. Despite being universally considered the reference for the dynamics of racing cars, Milliken [3] reports the torque bias diagram without any explanation. The featured LSD characteristics are symmetric on and off power, which is usually not the case. Among other renowned books [4] is the only one dealing extensively with LSD's and their impact on handling. Unfortunately, the beneficial effect in terms of stability off-power is totally missed as torque-sensitive systems are said to "act as free differentials on the overrun".

A relevant work is [16]: detailed modelling of the ramp differential internals is used to match a theoretical locking model with experimental data. Also Tremlett's work is focused on the impact of passive LSD's on the performance envelope of FWD and RWD racing cars [21-23; 26]. [23] in particular goes "back to basics" to explain the torque bias diagram. Dal Bianco et al. apply optimal control theory to the model of a single-seater racecar equipped with a LSD differential in [30]. Finally the passive LSD with its variants is dealt with extensively in [34].

Contemporary research is focused on active systems and assumes the basics of yaw control for granted. Among many papers, some that do recall the principles of a passive LSD are listed below. A significant contribution is [11] on the control strategy of the active limited-slip differential aimed at improving

handling and stability. Guidelines for tuning a passive LSD can be drawn as well. Three different situations arise according to driver demand, vehicle state and road conditions: steady state/power on, power off, and pure traction/ $\mu$ -split. An understeer curve (steering angle vs lateral acceleration) is also traced for open, limited-slip and semi-active differentials on the same car. Hancock's works is focused on yaw dynamics and control [8, 12-14, 18]. A comparison of active differential vs Rear Wheel Steering is dealt with in [5, 17].

By the way [3] classifies LSD adjustment as a secondary setup item in racing. Nowadays the diff is considered a primary one, while other factors should be added to the list of the secondary items, like suspension and steering friction [31, 32], the interaction between vertical and lateral loads in the steering system [28], as well as coupling effects between suspension non-linearities and downforce [33]. Again, although the LSD can also play a role in driverless experimental vehicles [25] its impact on driver workload can be a key to performance [27]. Differential locking also affects dynamics of the Vehicle Sideslip Angle [36].

### 3. BASIC PRINCIPLES

As it is always the case in vehicle dynamics, a good knowledge of tyre characteristics is required to understand the LSD. The typical shape of pure traction/braking force vs longitudinal slip and combined lateral and longitudinal forces are recalled in this section. A practical definition of the longitudinal slip is

$$s = \frac{\omega r - V}{\omega r} \text{ with } 0 \leq s \leq 1 \text{ on power} \quad (1)$$

$$s = \frac{\omega r - V}{V} \text{ with } -1 \leq s \leq 0 \text{ off power} \quad (2)$$

The longitudinal force vs slip curve can be seen in Fig. 1b. Only positive values (on power) are shown, assuming the negative slip curve is symmetric. For a given vertical load an almost linear zone is followed by a peak around  $s \approx 0.1$  then a strongly non-linear zone called saturation occurs: the tyre is not able to give further increments in terms of tractive force, as adhesion is superseded by slippage along the whole length of the tyre contact patch. The curves are scaled up for increasing vertical load, at least neglecting non-linear effects due to load sensitivity [20, 24].

#### 3.1 The spool

A simple form of final drive is the so-called spool. If there is no differential or if the differential is fully locked, both wheels are forced to rotate at the same angular velocity. The input power is equal to the output power and it is the same for the overall torque:

$$\omega_m = \omega_1 = \omega_2 \quad C_m = C_1 + C_2 \quad (3)$$

The torque bias i.e. the torque distribution on the drive wheels can only be determined by taking the longitudinal tyre characteristics into account, according to longitudinal slip ratio and vertical load. For a given speed and a given cornering radius, therefore in steady-state turning, the forward velocities of the outer and inner wheels depend upon the axle width  $c$  (Fig. 1a):

$$R_1 = R_2 + c \quad V_1 = \psi R_1 \quad V_2 = \psi R_2 \quad (4)$$

The following sections are aimed at explaining the impact of the spool on vehicle balance, handling and stability in an intuitive manner. Some assumptions are used for simplicity: the effect of combined tyre slip is dealt with separately for instance. Tyres are assumed to work in the linear range of the longitudinal force vs slip curve i.e. before the onset of saturation, and second-order effects (e.g. camber influence) are not considered.

#### 3.2 Steady-state and on-power cornering

According to the definition of longitudinal slip (1):

$$s_1 = \frac{\omega_1 r - \psi R_1}{\omega_1 r} \quad s_2 = \frac{\omega_2 r - \psi R_2}{\omega_2 r} \quad \omega_m = \omega_1 = \omega_2 \quad (5)$$

The tyre slip difference is determined by kinematics:

$$s_2 - s_1 = \frac{\omega_m r - \psi R_2}{\omega_m r} - \frac{\omega_m r - \psi R_1}{\omega_m r} = \frac{\psi(R_1 - R_2)}{\omega_m r} = \frac{\psi c}{\omega_m r} = \frac{Vc}{R\omega_m r} \quad (6)$$

$R_1 > R_2$  hence  $s_2 > s_1$ , and the inner wheel slip is larger. Now, assuming that lateral acceleration and lateral load transfer  $\Delta F_Z$  are negligible,  $F_{X2} > F_{X1}$  and a yaw moment is generated:

$$M_z = \Delta F_x \cdot c = (F_{X2} - F_{X1}) \cdot c \quad (7)$$

In agreement with [2], the yaw moment on power is an understeer (US) contribution. As this stabilizing effect is inversely proportional to the cornering radius it is particularly significant in tight cornering at very low speed: the spool will resist yaw rate therefore spoiling vehicle maneuverability, and friction at the contact patch will dissipate energy. When lateral acceleration is higher, the lateral load transfer  $\Delta F_Z$  is no longer negligible (Fig. 1b): the inner and outer tyres work on separate curves. The yaw moment is still towards US, but the amount is reduced.

Finally for extreme cornering speeds thus very high lateral acceleration, the lateral load transfer causes the inversion of the yaw moment, that becomes an oversteer (OS) contribution (Fig. 1c). On top of that when considering the combined tyre slip curves, a strong demand of tractive force will cause the outer tyre to shift towards higher slip angles [20, 24], thus further increasing the tendency to OS on a RWD car. This change in terms of vehicle balance can be unpredictable hence it is undesirable. In other words a spool makes the handling balance strongly affected by lateral acceleration and torque demand, generating US for low  $a_y$  and OS –probably associated with poor stability– for  $a_y$  levels close to the cornering limit.

#### 3.3 Off-power behaviour

Releasing the throttle means that the drive tyres will develop negative longitudinal forces due to the engine braking torque. Once again according to the definition of negative longitudinal slip (2), the slip difference is determined by kinematics:

$$s_1 = \frac{\omega_1 r - \psi R_1}{\psi R_1} \quad s_2 = \frac{\omega_2 r - \psi R_2}{\psi R_2} \quad \omega_m = \omega_1 = \omega_2 \quad (8)$$

$$s_2 - s_1 = \frac{\omega_m r - \psi R_2}{\psi R_2} - \frac{\omega_m r - \psi R_1}{\psi R_1} = \frac{\omega_m r}{\psi} \left( \frac{R_1 - R_2}{R_1 R_2} \right) = \frac{\omega_m r}{\psi} \left( \frac{c}{R_1 R_2} \right) \quad (9)$$

with  $R_1 > R_2$  and  $|s_1| > |s_2|$ . When lateral acceleration and load transfer  $\Delta F_Z$  are negligible, then  $|F_{X1}| > |F_{X2}|$  and an US moment, resisting yaw, is generated. In this case however even when lateral acceleration is higher there

is no inversion of the yaw moment, that remains on the US side (Fig. 1d).

A spool or locked differential always resists yaw even at very low speed, and unless the vehicle is driven close to the cornering limits. In this case the high lateral load transfer coupled with the demand of large tractive forces can result in an abrupt change of vehicle balance towards OS and instability. On the other side releasing the throttle in a corner is a critical situation for stability in itself [34], but in this case a locked differential always gives an US contribution promoting stability, sometimes at the expense of vehicle agility. The US yaw moment also increases yaw damping [13].

By the way a difference in longitudinal slip with the associated yaw moment is also generated in straight running on an uneven road surface, or whenever tyre pressure and rolling radius are different between the drive wheels. All the above makes the spool hardly compatible with the requirements of a road vehicle.

### 3.4 The open differential

The open or free differential is a well-known item universally adopted on ground vehicles to decouple the angular velocities of the drive wheels, thus avoiding the undesirable side effects of a spool. Assuming that energy losses due to internal friction and inertial terms are negligible, a symmetric differential is fully described by the following equations:

$$C_m = C_1 + C_2 \quad C_1 = C_2 = C_m/2 \quad \omega_m = \frac{\omega_1 + \omega_2}{2} \quad (10)$$

The open differential can therefore deliver torque to both wheels that remain free to rotate at different velocities, thus canceling tyre contact patch friction along a turn, and potentially achieving a condition close to pure rolling. The torque is always split into equal proportions left to right and does not interfere with cornering balance and driver inputs as no yaw moment is generated either on and off power.

A traction problem however is encountered whenever one of the tyres saturates for any reason. Two typical situations can be taken as reference examples:

1) Standing start on a  $\mu$ -split road surface: when a wheel is resting on a low-grip surface and can deliver limited or zero torque, neither this nor the other wheel can generate any torque/tractive force:

$$C_1 = C_2 = 0 \quad \omega_1 = 0 \quad \omega_2 = 2\omega_m \quad (11)$$

2) Acceleration in a corner with high lateral acceleration/load transfer: the inner wheel tends to lift off the ground and the tyre can saturate, developing low or null torque/tractive force. The same, limited amount of torque can be transmitted to the outer wheel (Fig. 2a):

$$C_1 = C_2 \cong 0 \quad S_1 \cong 0 \quad S_2 \cong 1 \quad (12)$$

$$\omega_1 \cong V/r \quad \omega_2 \cong 2\omega_m - V/r \quad (13)$$

The latter is quite common on RWD cars with a high power-to-weight ratio and a front-biased weight distribution. Even more so on FWD cars because of longitudinal load transfer on power. In any case whenever the inner wheel tends to spin, the open differential will prevent saturation of the outer tyre, allowing for enough lateral force to be generated with small slip angles hence restraining power US (FWD) or power OS (RWD).

### 3.5. Torque bias range: spool vs open differential

The differential working range can be traced on the so-called Torque Bias diagram, showing the left vs right output torques (Fig. 4a). The first quadrant corresponds to on-power operation ( $C_m > 0$ ) while the third one to off-power ( $C_m < 0$ ). The lines *AB* on power and *CD* off power represent the maximum input torque. The dotted line *MN* is the open diff. Equations are respectively

$$C_m = C_1 + C_2 \quad C_1 = C_2 = C_m/2 \quad (14)$$

*ABDC* is the working range of the spool with its typical "butterfly" shape. The torque bias is determined by vertical load and tyre slip and the entire torque can even be delivered to one wheel only. The line *BD* for instance means

$$C_1 = C_m = \Delta C_{MAX} \quad \text{and} \quad C_2 = 0 \quad (15)$$

### 4. THE LIMITED-SLIP OR SELF-LOCKING DIFF

The open differential is suitable for normal road vehicles, while the spool is only compatible with extreme applications [4]. A passive limited-slip device based on some sort of clutch in parallel with an open differential offers the potential to cover the entire working range between the open differential and the spool, with the related advantages (and disadvantages): it can be quite effective for high-performance vehicles like sports and racing cars, solving the traction problem and improving vehicle balance and stability at the same time. The open diff laws (10) are still applicable, in addition a dissipative device, based on friction, can bypass the bevel gears and deliver torque from the faster to the slower wheel through the diff case (Fig. 2b):

$$\omega_1 > \omega_2 \quad C_1 = C_m/2 - \Delta C \quad C_2 = C_m/2 + \Delta C \quad (16)$$

where  $\Delta C$  is the LSD locking torque. As stated previously the yaw moment affecting vehicle balance is

$$M_z = \Delta C \cdot \left( \frac{c}{r} \right) = \Delta F_x \cdot c \quad (17)$$

while the power balance shows that  $\Delta C$  is proportional to power loss through the clutch pack [10]:

$$\Delta C = \left( \frac{W_p}{\omega_1 - \omega_2} \right) \quad (18)$$

The simplest type of LSD is... the real-world open differential. The internal friction across the bevel gears can dissipate a certain amount of energy that is sensitive to either input torque and to wheel velocity difference, in a  $\mu$ -split situation for instance.

The more complex torque-sensitive, ramp-based differential and the effect of preload are explained extensively in the following sections, while the reader can refer to [4, 6, 34] for speed-sensitive devices.

#### 4.1. Torque-sensitive devices: a basic model

In this case the locking torque across the differential is proportional to the input torque:

$$\Delta C = f(C_m) \quad (19)$$

The most common torque-sensitive device on road-going sportscars and racing cars is the so-called ramp differential, often known as *Salisbury* or *Hewland Powerflow*<sup>®</sup> differential: with reference to Fig. 3, the differential case (2) transfers the torque to the satellite gear pins (6) by means of a pair of side rings (11). The torque is exchanged between each pin and a pair of

inclined surfaces called ramps (3). The wedging thrust tends to separate the side rings with a contact force proportional to the input torque and the cotangent of the ramp angle  $\sigma$ , pressing them against one or (usually) two wet clutch packs located between each ring and the differential carrier (8 and 9), that in turn develop the locking torque. Separate ramp pairs act on and off power, possibly with a different angle ( $\sigma = 60^\circ$  and  $30^\circ$  respectively in Fig. 3b). If the number of pins/ramp pairs  $n$  is 4, as in Fig. 3:

$$N_T = \frac{C_m}{8 \cdot r_{ramp}} \quad N_A = N_T \cdot \cot \sigma \quad F = 8N_A \quad (20)$$

and assuming the clutch packs work under uniform pressure distribution, the locking torque generated by the total axial thrust  $F$  on  $n$  clutch face pairs is

$$\Delta C = F \cdot \frac{2}{3} \cdot \left( \frac{R^3 - r^3}{R^2 - r^2} \right) \cdot n \cdot \mu_c = \frac{2}{3} \cdot \left( \frac{C_m}{r_{ramp}} \cdot \cot \sigma \right) \cdot \left( \frac{R^3 - r^3}{R^2 - r^2} \right) \cdot n \cdot \mu_c \quad (21)$$

This type of LSD is a versatile setup tool, especially for racing, as it is separately adjustable on- and off-power by changing the ramp angles. Also the number of clutch interfaces, acting as a torque multiplier, can be changed. The diagram in Fig. 4a is based on a motorsport differential with  $45^\circ/30^\circ$  ramps on and off power respectively and a 6-face wet clutch pack.

The working zones are defined by the following lines. On power the lines  $FO$  and  $EO$  correspond to the slower and faster wheel respectively:

$$C_{slowerW} = C_m/2 + \Delta C_{MAX} \quad C_{fasterW} = C_m/2 - \Delta C_{MAX} \quad (22)$$

while off power the lines  $HO$  and  $GO$  are the slower and faster wheel respectively:

$$C_{slowerW} = -|C_m/2 + \Delta C_{MAX}| \quad C_{fasterW} = -|C_m/2 - \Delta C_{MAX}| \quad (23)$$

where the maximum locking torque  $\Delta C_{MAX}$  is proportional to the input torque  $C_m$ . On- and off-power lines feature different gradients because of the different ramp angles in drive and overrun. The Torque Bias Ratio is defined as

$$TB = \frac{C_{slowerW\_MAX}}{C_{fasterW\_MAX}} \quad (24)$$

The ramp-based, torque-sensitive differential as a matter of fact can be tuned to cover the functional range between the spool and the free differential: the higher the torque bias ratio, the closer to a spool it becomes when input torque is applied. On the other side as the locking torque is directly proportional to the input torque, the unit is substantially a free differential during cruising and smooth driving, hence it is also suitable for road car applications. This is however also the main drawback: only limited or null input torque can be delivered on low friction and  $\mu$ -split surfaces, no locking arises and the traction problem occurs.

#### 4.2. The static preload

In order to handle the traction problem an axial preload is often applied statically to the clutch packs e.g. by means of a Belleville spring (10 in Fig. 3), resulting in a preload frictional torque across the diff. The effect or the preload alone is shown in Fig. 4b: for  $Q \leq C_m \leq P$  the differential is equivalent to a spool because the input torque  $C_m$  is not enough to overcome the preload, while for  $C_m < Q$  or  $C_m > P$ ,  $C_m$  has no

influence and  $\Delta C_{MAX} = P$ . The combination of ramp and preload results in a typical shape of the torque bias diagram defined by the  $\Delta C_{MAX}$  boundaries in Fig. 5a.

#### 4.3. Static and dynamic friction

The transition between static and dynamic friction can trigger instability of the clutch pack due to stick-slip oscillations, involving driveline torsional dynamics as well. An experimental study of the friction coefficient in wet clutch packs can be found in [21], showing that special lubricant additives can make static friction lower than dynamic friction and enable smooth operation of automatic transmissions. The usual assumptions related to friction physics are reversed. [13, 21] assume that the above is applicable to LSD clutch packs as well. Other sources [7, 12] however rely on traditional Coulomb's theory and Karnopp's modeling, in agreement with the authors' experience on motorsport transmissions. Static and dynamic friction coefficients can be respectively around  $\mu_S = 0.12$  and  $\mu_D = 0.08$  [9, 16]. Reference can be made to [34] for a detailed analysis of the transition.

#### 4.4. Additional locking effects

An experimental campaign on a motorsport unit [16] states that the axial load on the satellite gears is exchanged as wedging force between the gear back spherical face and the side rings, resulting into additional thrust on the clutch packs. Locking proportional to input torque is also provided by friction between the same back face and the side rings, and between the bevel teeth. These effects can be taken into account by means of a constant to be empirically determined:  $k \approx 0.08 \div 0.22$ . Considering also the pin/ramp friction coefficient  $\mu_R$  [23], (21) can be rearranged as

$$\Delta C = C_m \cdot \left[ k + \frac{2}{3} \cdot \left( \frac{n \cdot \mu_c \cdot \cos \sigma - \mu_R \sin \sigma}{r_{ramp} \cdot \sin \sigma + \mu_R \cos \sigma} \right) \cdot \left( \frac{R^3 - r^3}{R^2 - r^2} \right) \right] \quad (25)$$

#### 4.5. Setup variations

Typical ramp angles ranging from  $80^\circ$  (virtually no locking) to  $30^\circ$  (heavy locking) are usually available in different drive/overrun combinations. The locking action can be differentiated to a significant extent, and the whole range between a spool and a free differential can be covered. The adjustability range allows to address issues like braking and turn-in instability, often a problem of ground-effect racing cars. Care should be taken with the amount of preload: too much usually means turn-in and/or mid-corner US, not enough might trigger the traction issue in corner exit. Diffs with externally adjustable preload are often used on racecars.

Other variants of the torque-sensitive LSD such as the negative preload, the VCP (Viscous Coupling Plate) and the *Torsen*<sup>®</sup> are described in [9, 15, 34].

### 5. TESTING AND SIMULATION EXAMPLES

As stated above [29] seems to be the only experimental work showing a real-world torque bias diagram. Output torque data have been measured by means of Kistler wheel force transducers on a production-based racing car. In the second example, a full GT racing car model was built in *VI-CarRealTime*<sup>®</sup>, a parametric software dedicated to vehicle dynamics [35]. The LSD model was built as shown in the previous

sections. Fig. 5b shows the torque bias diagram for a single lap on the Imola circuit.

The diagram is mapped on input torque. The whole working zone is used, apart from an “empty” area for low torque input values. The diff acts as a spool quite often, either in the preload and in the ramp regions, and the ramp setting off power is quite aggressive in this case to improve braking and turn-in stability.

## 6. CONCLUSION

The paper recaps the effects of the passive limited-slip differential on handling, traction, stability, and ultimately performance by generation of a yaw moment, as a basis to better understand the principles of torque vectoring. A simple model is presented for the torque-sensitive differential and the torque bias diagrams are discussed. The results of specific vehicle dynamics simulations are presented briefly.

## REFERENCES

- [1] Lorenz, K.; Dietrich, C.; Donges, E. (1986). Einfluss des sperrdifferentials auf traction und fahrverhalten von fahrzeugen in standardbauweise, teil 1 und 2. *Automobiltechnische Zeitschrift*, 88 (2), 95-100 and (3) 149-153.
- [2] Mastinu, G. et al. (1993). The influence of limited-slip differentials on the stability of rear-wheel-drive automobiles running on even road with dry surface. *Int. J. of Vehicle Design*, 14 (2/3), 166-183.
- [3] Milliken, W.F.; Milliken, D.L. (1995). *Racecar Vehicle Dynamics*. SAE International.
- [4] Dixon, J.C. (1996). Tyres, suspension and handling, second edition. SAE International.
- [5] Abe, M. et al. (1996). A direct yaw moment control for improving limit performance of vehicle handling – comparison and cooperation with 4WS. *Vehicle System Dynamics (Suppl. 25)*, 3-23.
- [6] Huchtkoetter, H.; Klein, H. (1996). The effect of various limited-slip differentials in front-wheel-drive vehicles on handling and traction. *Transmission and Driveline Systems Symposium: Efficiency, Components, and Materials*, Detroit, JAE paper, 960717, 131-141.
- [7] Deur, J.; Asgad, J.; Hrovat, D. (2000). Modelling of CD4E Planetary Gear Set Based on Karnopp Model for Clutch Friction. Ford Research Laboratories.
- [8] Hancock, M.; Best, M. et al. (2005): A comparison of braking and differential control of vehicle yaw-sideslip dynamics. *Proc. of the IMechE: Part D: J. of Automobile Engineering* 219, 309–27.
- [9] Xtrac Ltd. 379 gearbox manual, 2005.
- [10] Cheli, F. (2006). *Vehicle Mechanics Lecture notes*, Politechnic of Milan.
- [11] Cheli, F. et al. (2006). Development of a new control strategy for a semi-active differential for a high-performance vehicle. *Vehicle System Dynamics*, 44 (sup1): 202-215.
- [12] Hancock, M.J. (2006). *Vehicle handling control using active differentials*. PhD thesis.
- [13] Hancock, M.J.; Williams, R.A.; Fina, E.; Best, M.C. (2007). Yaw motion control via active differentials. *Transactions of the Institute of Measurement and Control*, 29 (2): 137-157.
- [14] Assadian, F.; Hancock, M.; Best, M.C. (2008). Development of a control algorithm for an active limited slip differential. In: *Proc. of the 10th Int. Symposium on Advanced Vehicle Control (AVEC)*; Loughborough (UK); 2008. p. 55–60.
- [15] Hewland Eng. Ltd. EMA differential manual, 2008.
- [16] Dickason, I. (2009). Development of a theoretical locking model for a motorsport mechanical plate differential. Master thesis, Cranfield University.
- [17] Canale, M.; Fagiano, L. (2010). Comparing rear wheel steering and rear active differential approaches to vehicle yaw control. *Vehicle System Dynamics*, 48 (05): 529-546.
- [18] Deur, J.; Hancock, M. et al. (2010). Modeling and analysis of active differential dynamics. *ASME, J Dyn Syst Measurement Control*. 2010; 132.
- [19] Ingram, M. et al. (2011). Frictional properties of automatic transmission fluids: Part I – measurement of friction sliding speed behaviour. *Tribol Trans* 54 (1): 145-153.
- [20] Pacejka, H.B. (2012). *Tyre and vehicle dynamics*. SAE International.
- [21] Tremlett, A.J. et al. (2012). The influence of torque and speed sensitive differential characteristics in a FWD vehicle during on limit manoeuvres. *Proc. of the FISITA 2012 World Automotive Congress, Lecture Notes in Electrical Engineering*, Beijing, China. Berlin, Heidelberg: Springer. 193, 79-91.
- [22] Tremlett, A.J. et al. (2012). The control authority of passive and active torque vectoring differentials for motorsport applications. *Proc. of the FISITA 2012 World Automotive Congress, Lecture Notes in Electrical Engineering*, Beijing, China. Berlin, Heidelberg: Springer. 193, 335-347.
- [23] Tremlett, A.J. et al. (2014). Quasi steady state linearisation of the racing vehicle acceleration envelope: a limited slip differential example. *Vehicle System Dynamics*, 52 (11): 1416-1442.
- [24] Guiggiani, M. (2014). *The science of vehicle dynamics*. Springer.
- [25] Chindamo, D. et al. (2014). A neurofuzzy-controlled power management strategy for a series hybrid electric vehicle. *Proc. of the IMechE, Part D: J. Automobile Engineering*, 228 (9), 1034-1050.
- [26] Tremlett, A.J. et al. (2015). Optimal control of motorsport differentials. *Vehicle System Dynamics*, 53 (12): 1772-1794.
- [27] Crema, C.; Depari, A.; Flammini, A.; Vezzoli, A.; Benini, C.; Chindamo, D.; Gadola, M.; Romano, M. (2015). Smartphone-based system for vital parameters and stress conditions monitoring for non-professional racecar drivers. *Proc. of the 2015 IEEE SENSORS*. 7370521.
- [28] Marchesin, F.P.; Barbosa, R.S.; Alves, M.A.L.; Gadola, M.; Chindamo, D.; Benini, C. (2016). Upright mounted pushrod: the effects on racecar handling dynamics. *The Dynamics of Vehicles on Roads and Tracks. Proc. of the 24th Symposium of the International Association for Vehicle System Dynamics, IAVSD 2015*. 543-552.

[29] Rouelle, C.; Kloppenborg, S. (2016). Differential behaviour. OptimumG, lecture notes.

[30] Dal Bianco, N.; Lot, R.; Gadola, M. (2017). Minimum time optimal control simulation of a GP2 race car. Proc. of the IMechE, Part D: J. of Automobile Engineering.

[31] Gritti, G.; Peverada, F.; Orlandi, S.; Gadola, M. et al. (2017). Mechanical steering gear internal friction: effects on the drive feel and development of an analytic experimental model for its prediction. Proc. of the Intl. Joint Conf. on Mechanics, Design Eng. & Adv. Manufacturing (JCM), Catania, Italy.

[32] Benini, C; Gadola, M; Chindamo, D et al. (2017). The influence of suspension components friction on race car vertical dynamics. Vehicle System Dynamics. 55 (3): 338-350.

[33] Marchesin, F.P.; Barbosa, R.S.; Gadola, M.; Chindamo, D. (2017). High downforce racecar vertical dynamics: aerodynamic index, Vehicle System Dynamics, 2017, in press.

[34] Gadola, M. (2017). Lecture notes on self-locking differentials and 4-wheel-drive traction.

[35] Bettinsoli, S.; Leali, G. (2018). Studio e modellazione dinamica di una vettura da competizione Lamborghini Huracán GT3 tramite software VI-CarRealTime. Degree Thesis, University of Brescia.

[36] Chindamo, D.; Lenzo, B.; Gadola, M. (2018). On the vehicle sideslip angle estimation: a literature review of methods, models and innovations. Appl. Sci. 2018, 8(3), 355.

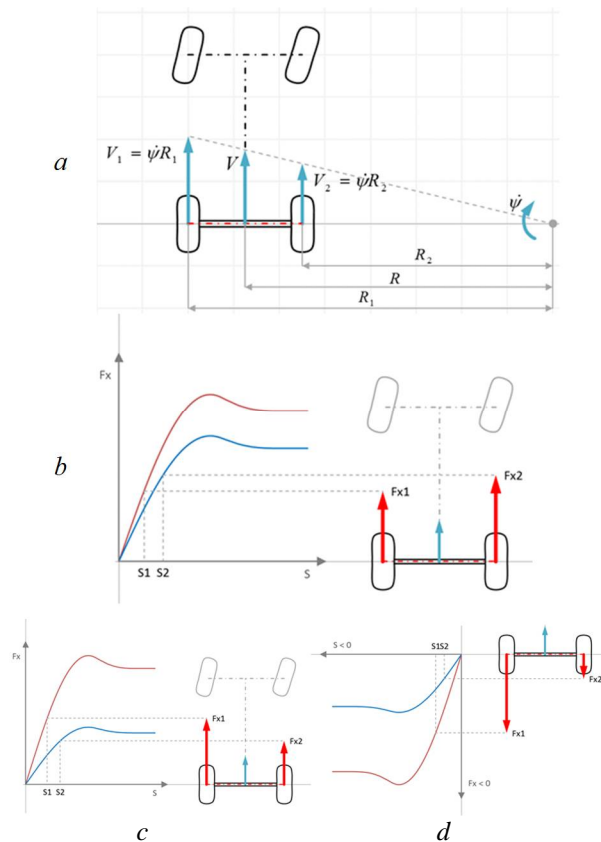


Fig. 1 Spool effects on a RWD car: a) forward velocities of the driven wheels, b) US on power, c) OS in high-speed cornering, d) US off power, high-speed cornering

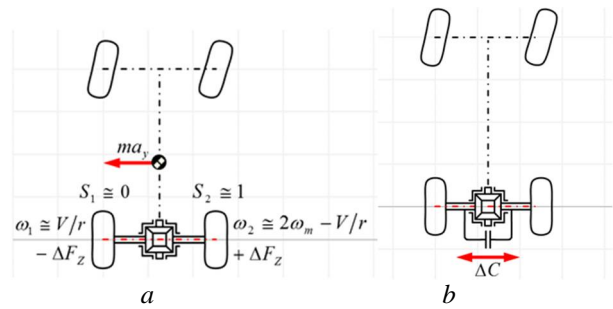


Fig. 2 a) traction limitation on  $\mu$ -split road surface with open differential; b) generic LSD

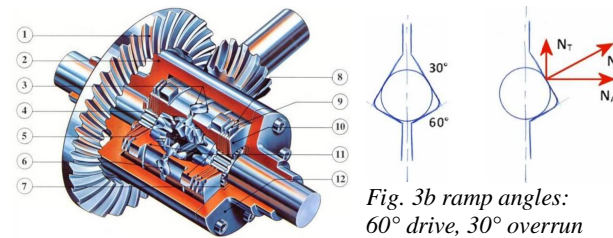


Fig. 3 The ramp LSD (courtesy ZF). 1) crown&pinion, 2) diff carrier, 3) ramp pair on side gear rings, 4) satellite bevel gears (spider gears), 5) driven bevel gears, 6) satellite gear pin, 7) spline gear, output shaft, 8) clutch disks coupled with output shaft, 9) clutch disks coupled with diff carrier, 10) Belleville spring for axial preload, 11) side gear pressure rings, 12) housing cover

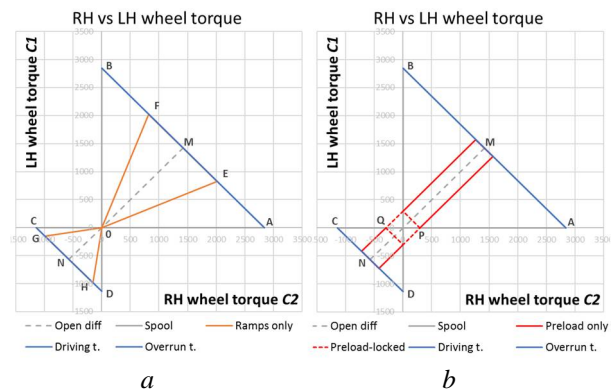


Fig. 4 LH vs RH output torque bias diagram: a) 45°/30° ramps, no preload, 6 clutch disk faces b) preload only

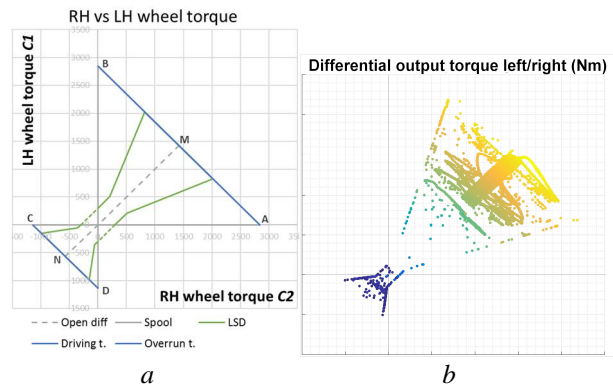


Fig. 5 LH vs RH output torque bias diagram: a) ramp and preload effects combined b) vehicle dynamics model of a GT racecar, lap time simulation